ISBN: 978-3-95450-247-9 ISSN: 2673-5490 doi: 10.18429/JACoW-IPAC2024-THPS21

STRAIN MEASUREMENTS OF THE APPLE-X SABINA UNDULATOR WITH FIBER BRAGG GRATING

I. Balossino[1] *, M. Caponero[2], M. Del Franco[1], E. Di Pasquale[1], L. Giannessi[1], F. Nguyen[2], A. Petralia[2], A. Polimadei[2], L. Sabbatini[1], A. Selce[1], A. Vannozzi[1]
[1]INFN National Laboratory of Frascati, Rome, Italy, [2]ENEA Frascati, Rome, Italy

Abstract

SABINA (Source of Advanced Beam Imaging for Novel Applications) is a new IR/THz FEL source under construction at the INFN Laboratori Nazionali di Frascati (LNF). The FEL is a single-pass amplifier designed to operate in the 10-100 THz spectral range using the SPARC infrastructure. The amplifier, consisting of three Apple-X undulator modules built by KYMA S.p.a, will deliver pulse energies of tens of microJoule with variable polarisation.

The undulators were delivered to LNF in 2023. In collaboration with ENEA, the mechanical structure was investigated for stability and deformations, by strain measurements based on Fiber Bragg Gratings (FBG). An FBG is a phase grating inscribed in the core of a single-mode fiber, whose Bragg-diffracted light propagates back along the fiber. Any deformation of the grating affects its pitch, which changes the diffracted Bragg wavelength thus giving information about the occurred deformation. The technique allows performing strain measurements with 1 μStrain resolution. Each undulator has four magnetic arrays that can be moved radially to set the operating gap. Two arrays can also move longitudinally for phase displacement. Measurements have been performed with FBGs acting as strain sensors on the undulator structure. The measurements have shown a clear deformation of the structure in the presence of varying magnetic forces. The results will be presented in this contribution.

RESEARCH CONTEXT

SABINA [1] is a project developed at the Frascati National Laboratories (LNF) of the Italian Institute of Nuclear Physics (INFN) co-funded by the Lazio Region. It aims to upgrade the already existing SPARC_LAB research facility [2] that will be completed with EuPRAXIA@SPARC_LAB [3] in the next future.

SABINA

The project was initiated as part of a regional call for the development of research infrastructures. It foresees the realization of a research facility that will be made available to external users, whether they are researchers or from other industrial or technological backgrounds. In order to achieve these objectives several steps were required to ensure the reliability of the SPARC accelerator: consolidation of the technological equipment to limit the faults and increase the uptime; replacement of some ancillary equipment with modern equipment to improve the overall performance: implementation of two user lines, a laser target line and a THz/IR radiation line. The former will be used as an irradiation facility for samples such as vacuum optics for aerospace, while the latter will be used as a research tool for various fields. The radiation will be generated by the undulators which are the main subject of this paper.

THz/IR line

The THz/IR free-electron laser source uses the high-brightness electron beam generated by the photocathode at SPARC LINAC and tuned to energies between 30 and 100 MeV. A dogleg directs the beam to the THz/IR amplifier which consists of three APPLE-X undulators operating in self-amplified spontaneous emission (SASE) mode in the spectral range from 3 to 30 THz. The amplifier is expected to generate pulses with variable polarisation, picosecond duration, and an energy of tens of μJ. A dedicated THz transport line delivers photons to a user's experimental area. The facility will allow non-invasive investigation studies for both research and industrial applications in several fields, from physics to chemistry, material science, and cultural heritage.

EXPERIMENTAL SETUP

The undulators were designed and produced by KYMA S.p.a. [4] in accordance with the requirements and constraints of the INFN technical specification. During the design phase, a thorough structural analysis was performed on critical elements to validate the lightweight design of this application. The result is an innovative, compact, and lightweight design of an Apple X-type undulator. A test of the mechanical structure deformations has been carried out on the mechanical structure by strain measurements, with the support and use of Fiber Bragg Grating instrumentation of the ENEA Fiber Optic Sensors Laboratory [5].

APPLE-X Undulator

The undulator [6] consists of four magnetic arrays mounted on identical magnetic girders, which are fixed to the guide rail carriages of the gap drive mechanism (see Fig. 1). The gap between the arrays can be varied by simultaneous movements of the girders hosting the magnets. Two of the four arrays, positioned diagonally, can also be moved longitudinally to induce a field phase displacement between the arrays of half a period. Each magnet block is precisely positioned on a magnet holder. Along the length of the array, the magnet holders are screwed on top of three aluminum plates. These latter are then sustained by one interface plate

* ilaria.balossino@lnf.infn.it

ISBN: 978-3-95450-247-9 ISSN: 2673-5490 doi: 10.18429/JACoW-IPAC2024-THPS21

towards the girder. The three holder plates and the interface plate are shown in Fig. 1 and are the structures under investigation.

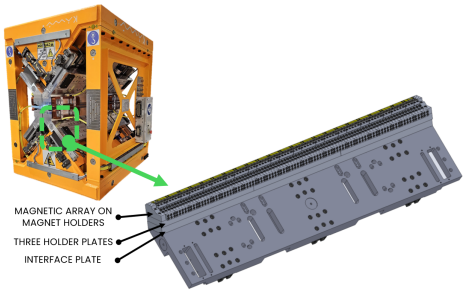

Figure 1: Mechanical structure under investigation.

Fiber Bragg Grating Sensors

The Fiber Bragg Grating (FBG) [7] is an optical fiber sensor in which a periodic microstructure is locally photo-inscribed to create a diffraction grating with the desired optical properties. The periodic change in the fiber refractive index determines the transmitted/reflected spectrum of the light passing through the fiber core. Any deformation of the grating is detected as a shift in the characteristic wavelength of the sensor. The selected sensors were 1 cm long (Broptics OS 1500 optical sensors) and were used with Micron Optics FBG interrogation instruments [8]. The sensors were bonded to the surfaces facing the inside part of the undulator using Araldite epoxy adhesives. The plotted parameter is the wavelength shift induced by the deformation of the fiber. The wavelength shift $\Delta\lambda$ can be converted into a strain parameter considering that 1 strain (= 1 µm/m) of deformation corresponds to $\Delta\lambda = 1.2$ pm. These sensors were used in two different ways: as *strain measurements*, by gluing the fiber fully adhered to the surface of the magnet holder-plates; as *gap measurement* devices, by placing the sensors between adjacent plates. In both cases the measurement is local, but in the first case, the reference length is the length of the sensor. In the second case, the reference length is the separation between the adjacent plates. The two undulator arrays allowed to shift longitudinally were considered. A total of 28 sensors have been used, as shown in Fig. 2:

- 1 FBG to monitor the temperature of the environment
- 20 FBGs placed between metal bars (*gap sensors*)
- 7 FBGs completely adherent to the metal (*strain sensors*)

RESULTS

The results of these kinds of measurements can not be unambiguous and clear since the FBG reacts both at a deformation of the grating itself due to temperature changes and at the mechanical movements of the element under investigation. The most relevant results are shown in the next paragraphs.

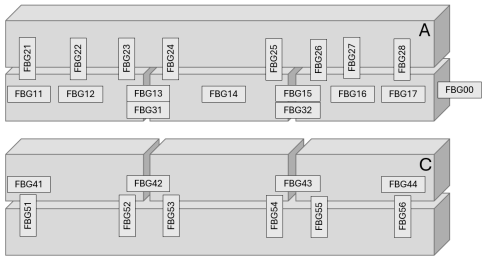

Figure 2: FBG placement on the mechanical plates of two diagonal plates. "A" is the top array with longitudinal movements, "C" is the bottom one.

Environment

A static measurement was carried out over a time interval of 22 hours. During this period the environment temperature varied by about $3°C$ (see Fig. 3a). FBG sensors are sensitive to the temperature. The dependence of the strain measured as a function of the temperature is shown in Fig. 3b.

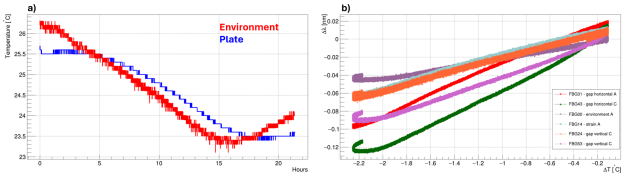

Figure 3: a) Temperature sensors. *RED*, is the sensor close to the undulator that gives the environment trend; *BLUE* is the sensor adherent with the metal close to the Environment FBG sensor. b) FBG sensors results for a different kind of investigation.

The maximum variation is found in the horizontal gap sensor in the lower array, while the minimum variation is found in the sensor completely adhering to the metal plate, but on the outer part of the undulator. This indicates that the *gap sensors* which mainly measure the empty space between the plates undergo a more significant change with respect to the others, which are sensitive to the thermal expansion of the metal part.

Gap Opening

This test was performed in two ways: by moving the four arrays all together from the minimum gap to the maximum gap, and in small steps from minimum gap to 50 mm of gap opening. The two sets of plots represent both measurements for a chosen set of sensors relevant to this study. The remaining sensors have shown negligible strain values and have been excluded from the plots. Figure 4, shows the full operation in the measurement range where the undulator goes from fully closed (5 mm) to fully open (150 mm) with a velocity of the arrays of 1 mm/s. The measurements are separated in terms of the orientation of the sensor. The left plot shows sensors oriented vertically, while the right plot shows horizontally oriented sensors. Figure 5 shows the same parameters acquired by progressively opening and closing the

ISBN: 978-3-95450-247-9 ISSN: 2673-5490 doi: 10.18429/JACoW-IPAC2024-THPS21

gap in steps of 5 mm, every two minutes each. The total measurement time was less than one hour. For this reason, the measurement should be unaffected by environmental temperature variations.

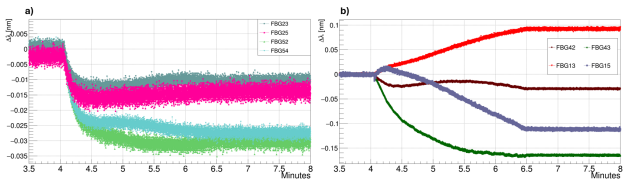

Figure 4: a) Vertical sensors. b) Horizontal sensors. Note that the y-axes are not on the same scale to appreciate the behavior of the vertical sensors. The movements performed are undulator fully closed on the left part of each plot, and fully open on the right part of each plot.

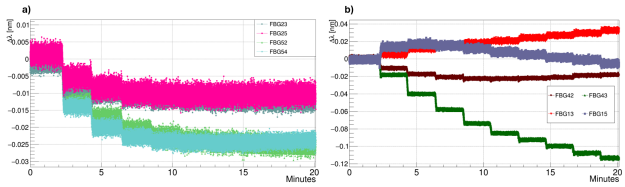

Figure 5: a) Vertical sensors. b) Horizontal sensors. Note that the y-axes are not on the same scale to appreciate the behavior of the vertical sensors. The movement shown is from undulator fully closed on the left part of each plot, and at 50 mm on the right part of each plot. Each noticeable step corresponds to a movement of 5 mm.

The maximum deformation with respect to the closed gap condition, is reached at a gap of about 20 mm. The horizontal sensors plotted on the right show a different behavior and a larger deformation. It is interesting to note that in the first phase of the gap aperture, the sensors on the top array (FBG13 and FBG15) go in opposite directions with respect to the other sensors (FBG42 and FBG43). When the distance reaches about 20 mm the trend changes for FBG15 and FBG42. A possible explanation is that when the magnetic force becomes weaker the central plate moves laterally causing the two sensors on the same array to indicate strains in opposite directions. If a gap sensor is stretched, the other is compressed. FBG42 shows an additional change in the strain before reaching the plateau corresponding to the maximum aperture, which is probably related to the effect of the sum of magnetic and gravitational forces that change sign.

Phase Shifting

The shift of the phase of the field is obtained by translating longitudinally the two arrays that are monitored with FBGs. A further test, similar to the gap opening, was carried out by shifting the phase at different undulator gaps. In Fig. 6 the effect of a phase shift with the undulator tuned at minimum gap is shown. This corresponds to the condition with the maximum magnetic forces. The phase shift causes a strain in the horizontal sensors only slightly higher than in other measurements (Fig. 6b). The strain is symmetric with respect to the phase, i.e. setting the phase at $\pm\frac{\lambda}{2}$ induces the same strain reaction. All the vertical sensors (Fig. 6a) still show a variation but correspond to a relatively small strain.

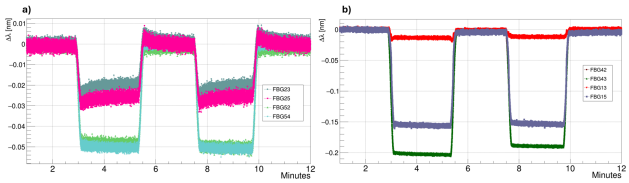

Figure 6: a) Vertical sensors. b) Horizontal sensors. Note that the y-axes are not on the same scale to appreciate the behavior of the vertical sensors. The movements are performed with the undulator closed, shifting the phase from 0 to almost $\frac{\lambda}{2}$ then 0, to almost $-\frac{\lambda}{2}$ then 0 again.

CONCLUSION

The largest observed wavelength shift is ~0.2 nm for the gap sensors and a factor 2-5 lower for the strain sensor devices. In the case of the gap sensors,the reference length is the plates separation. We may then estimate a gap variation of about 167 nm (over a 1 mm gap). In the case of the strain sensor, the deformation occurs over the entire sensor length. The local deformation is therefore of the order of 330 nm/cm. These measurements show the extreme sensitivity of this diagnostic. The deformations are compatible or lower than those calculated by finite elements methods [6] and confirm the reliability of the undulator mechanical structure.

ACKNOWLEDGEMENTS

This work is supported by NextGeneration EU- Italian National Recovery and Resilience Plan, Mission 4 - Component 2 - Investment 3.1. - Project name: Rome Technopole, CUP: I93C21000150006. SABINA is a project co-funded by Regione Lazio with the “Research infrastructures” public call within PORFESR 2014-2020.

REFERENCES

[1] L. Sabbatini *et al.*, “SABINA: A Research Infrastructure at LNF”, in *Proc. IPAC’21*, Campinas, Brazil, May 2021, pp. 4505–4507. doi:10.18429/JACoW-IPAC2021-THPAB372

[2] M.Ferrario *et al.*, “SPARC_LAB present and future”, *Nucl. Instrum. Methods Phys. Res., Sect. B*, vol. 309, pp. 183–188, Aug. 2013. doi:10.1016/j.nimb.2013.03.049

[3] M.Ferrario *et al.*, “EuPRAXIA@SPARC_LAB Design study towards a compact FEL facility at LNF”, *Nucl. Instrum. Methods Phys. Res., Sect. A*, vol. 909, pp. 134–138, Nov. 2018. doi:10.1016/j.nima.2018.01.094

[4] KYMA S.p.a, https://kyma-undulators.com/.

[5] ENEA Frascati, https://www.ricercanucleare.enea.it/.

[6] J. Počkar *et al.*, “Design of the Innovative Apple-X AX-55 for SABINA Project, INFN Laboratori Nazionali di Frascati”, in

ISBN: 978-3-95450-247-9 ISSN: 2673-5490 doi: 10.18429/JACoW-IPAC2024-THPS21

Proc. FEL'22, Trieste, Aug. 2022, pp. 475-478. doi:10.18429/JACoW-FEL2022-WEP47

[7] K. T. V. Grattan and T. Sun, "Fiber optic sensor technology: an overview", *Sens. Actuators, A*, vol. 82, no. 1–3, pp. 40–61, May 2000. doi:10.1016/s0924-4247(99)00368-4

[8] FBG sensors datasheet, http://www.broptics.com/products_sensor.htm/.